ARTICLE IN PRESS

Alexandria Engineering Journal (2020) **xxx**, xxx–xxx

HOSTED BY

ELSEVIER

Alexandria University

Alexandria Engineering Journal

www.elsevier.com/locate/aej
www.sciencedirect.com

The transient analysis for zero-input response of fractal RC circuit based on local fractional derivative

Kang-Jia Wang [a], **Hong-Chang Sun** [b,c,*], **Zhe Fei** [c]

[a] *School of Physics and Electronic Information Engineering, Henan Polytechnic University, Jiaozuo 454003, China*
[b] *School of Control Science and Engineering, Shandong University, Jinan 250061, China*
[c] *Shandong Dawei International Architecture Design Co., Ltd., Jinan 250101, China*

Received 6 March 2020; revised 21 July 2020; accepted 21 August 2020

KEYWORDS

Local fractional calculus;
Local fractional derivative;
Zero-input response;
Fractal circuit systems

Abstract Local fractional calculus has gained wide attention in the field of circuit design. In this paper, we propose the zero-input response(ZIR) of fractal RC circuit modeled by local fractional derivative(LFD) for the first time. With help of the law of switch and the Kirchhoff Voltage Laws, the transient local fractional ordinary differential equation is established, and the corresponding exact solution behavior defined on Cantor sets is presented. What we found especially interesting was that the fractal RC becomes the ordinary one in the particular case $\kappa = 1$. The results obtained in this paper reveal that the local fractional calculus is a powerful tool to analyze the fractal circuit systems.

1. Introduction

The theory of fractional calculus [1–4], emerging as a powerful mathematical analysis tool, has been successfully used to model the non-differentiable(ND) and fractal phenomena in science and engineering. For example, Kumar D, et al. proposed the fractional exothermic reactions model in porous media in [5]. Ghamisi et al. studied the segmentation of images using fractional calculus in [6]. Yu et al. discussed the fractal characters of porous media in [7]. Goswami et al. presented an efficient solution for the fractional equal width equation arising in cold plasma [8]. Atangana discussed the nonlinear Fishers reaction–diffusion equation in [9]. Markup et al. analysed the fractional vibration equation in [10]. Kumar et al. proposed the fractional epidemiological model of computer viruses in [11]. Baleanu et al. given an exact solution for wave equations on cantor sets in [12]. Bhatter et al. investigated the fractional Drinfeld-Sokolov-Wilson model in [13]. Dubey et al. studied the time fractional partial differential equations in [14]. And more applications in other fields are referred to [15–23]. Recently, a new definition of LFD has attracted much attention in various fields and is successfully applied to describe many ND phenomena, such as Korteweg-de Vries equation [24], rheological [25], circuits [26,27], nonlinear Burgers equation[28], Boussinesq equation [29], nonlinear local fractional

* Corresponding author at: School of Control Science and Engineering, Shandong University, Jinan 250061, China and Shandong Dawei International Architecture Design Co., Ltd., Jinan 250101, China.
E-mail address: hongchangs@126.com (H.-C. Sun).

Peer review under responsibility of Faculty of Engineering, Alexandria University.

https://doi.org/10.1016/j.aej.2020.08.024
1110-0168 © 2020 Faculty of Engineering, Alexandria University. Production and hosting by Elsevier B.V.

PDEs [30], vibration [31], filter [32], nonlinear local fractional PDEs [33] and so on [34–38].

The main aim of this paper is to present the ZIR of fractal RC circuit using LFD inspired by recent work in the fractal circuits. The structure of this paper is arranged as follows. In Section 2, we introduce the definitions and properties of the LFD, local fractional Laplace transform(LFLT) and inverse local fractional Laplace transform(ILFLT). In Section 3, we define the ND capacitor and ND resistor by LFD, and introduce the Kirchhoff Voltage Laws. In Section 4, the ZIR of fractal RC circuit is proposed by using the law of switch, and the corresponding solution on Cantor sets is presented. In Section 5, we give the analysis of the ZIR in detail. Finally, the conclusion is drawn in Section 6.

2. The correlative theories

Definition 2.1. For $\forall \varepsilon > 0, \delta > 0$ and $0 < |\tau - \tau_0| < \delta$, if there is [39]:

$$|\Xi(\tau) - \Xi(\tau_0)| < \varepsilon^{\kappa},$$

We say that $\Xi(\tau)$ is a local fractional continuous function with a fractal dimension κ, or $\Xi(\tau) \in C_{\kappa}(\omega, \varpi)$, where $C_{\kappa}(\omega, \varpi)$ is a set of local fractional continuous functions in the interval (ω, ϖ).

Definition 2.2. Let $\Xi(\tau) \in C_{\chi}(\omega, \varpi)$, the LFD of the function $\Xi(\tau)$ of order $\kappa (0 < \kappa \leqslant 1)$ is defined as [39]:

$$\Xi^{(\kappa)}(\tau_0) = \frac{d^{\kappa}\Xi(\tau)}{d\tau^{\kappa}}|_{\tau=\tau_0} = \lim_{\tau \to \tau_0} \frac{\Delta^{\kappa}(\Xi(\tau) - \Xi(\tau_0))}{(\tau - \tau_0)^{\kappa}}, \tag{2.1}$$

where $\Delta^{\kappa}[\Xi(\tau) - \Xi(\tau_0)] \cong \Gamma(1+\kappa)[\Xi(\tau) - \Xi(\tau_0)]$. By letting $\Xi^{(\kappa)}(\tau) = D_{\tau}^{\kappa}\Xi(\tau)$, then the LFD of higher order can be expressed as:

$$\Xi^{(m\kappa)}(\tau) = \underbrace{D_{\tau}^{\kappa} \dots D_{\tau}^{\kappa}}_{m \ times} \Xi(\tau) \tag{2.2}$$

Definition 2.3. The Mittag–Leffler function, sine function and cosine function on Cantor sets with a fractal dimension κ are defined as follows[39]:

$$E_{\kappa}(\tau^{\kappa}) = \sum_{p=0}^{\infty} \frac{\tau^{p\kappa}}{\Gamma(1 + p\kappa)} \tag{2.3}$$

$$sin_{\kappa}(\tau^{\kappa}) = \sum_{p=0}^{\infty} (-1)^p \frac{\tau^{(2p+1)\kappa}}{\Gamma[1 + (2p+1)\kappa]} \tag{2.4}$$

$$cos_{\kappa}(\tau^{\kappa}) = \sum_{p=0}^{\infty} (-1)^p \frac{\tau^{2p\kappa}}{\Gamma[1 + (2p+1)\kappa]} \tag{2.5}$$

where $p \in N$, the LFDs of several functions are listed in Table 1.

Definition 2.4. If the LFLT of function $\Xi(\tau)$ denoted by $\wp_{\kappa}[\Xi(\tau)] = N_{\kappa}^{\Xi}(\chi)$, the LFLT is defined as [39]:

$$\wp_{\kappa}[\Xi(\tau)] = N_{\kappa}^{\Xi}(\chi) = \frac{1}{\Gamma(1+\kappa)} \int_0^{\infty} \Xi(\tau) E_{\kappa}(-\tau^{\kappa}\chi^{\kappa})(d\tau)^{\kappa} \tag{2.6}$$

Table 1 The LFDs of several functions on Cantor sets.

$\Xi(\tau)$	$\Xi^{(\kappa)}(\tau)$
p	0
$E(p\tau^{\kappa})$	$pE(p\tau^{\kappa})$
$\frac{\tau^{p\kappa}}{\Gamma(1+p\kappa)}$	$\frac{\tau^{(p-1)\kappa}}{\Gamma(1+(p-1)\kappa)}$
$cos_{\kappa}(p\tau^{\kappa})$	$-psin_{\kappa}(p\tau^{\kappa})$
$sin_{\kappa}(p\tau^{\kappa})$	$pcos_{\kappa}(p\tau^{\kappa})$

where $\wp_{\kappa}$ is called the LFLT operator.

Theorem 1. *Suppose that the LFLT of $\Xi(\tau)$ is denoted by $\wp_{\kappa}[\Xi(\tau)] = N_{\kappa}^{\Xi}(\chi)$. Then we have*

$$\wp_{\kappa}\left[\Xi^{(i\kappa)}(\tau)\right] = \chi^{i\kappa}\wp_{\kappa}[\Xi(\tau)] - \sum_{j=0}^{i-1} \chi^{(i-1-j)} \Xi^{(i\kappa)}(0). \tag{2.7}$$

where $i, j \in N$, and $\Xi^{i\kappa}(\tau)$ is the LFD of order $i\kappa$. The LFLTs of several functions are listed in Table 2.

Definition 2.5. The definition of inverse local fractional Laplace transform(ILFLT) of $N_{\kappa}^{\Xi}(\chi)$ is given as

$$\Xi(\tau) = \frac{1}{(2\pi)^{\kappa}} \int_{\beta - i\omega}^{\beta + i\omega} N_{\kappa}^{\Xi}(\chi) E_{\kappa}(\tau^{\kappa}\chi^{\kappa})(d\chi)^{\kappa} \tag{2.8}$$

where $\chi = \beta + i\omega, \chi^{\kappa} = \beta^{\kappa} + i^{\kappa}\omega^{\kappa}$ and $\omega \to \infty$.

3. The ND lumped elements within LFD

3.1. The ND capacitor

The expression which describes the constitutive relation between the ND charge $\Phi_{\kappa}(\tau)$ and ND current $i_{\kappa}(\tau)$ within the LFD reads as

$$i_{\kappa}(\tau) = \frac{\partial^{\kappa}\Phi_{\kappa}(\tau)}{\partial\tau^{\kappa}} \tag{3.1}$$

Definition 3.1. The capacitance of ND capacitor is given as

$$C_{\kappa} = \frac{\Phi_{\kappa,C}(\tau)}{U_{\kappa,C}(\tau)} \tag{3.2}$$

Table 2 The LFLTs of several functions on Cantor sets.

$\Xi(\tau)$	$\wp_{\kappa}[\Xi(\tau)]$
1	$\frac{1}{\chi^{\kappa}}$
$E(a\tau^{\kappa})$	$\frac{1}{\chi^{\kappa}-a}$
$\frac{\tau^{p\kappa}}{\Gamma(1+p\kappa)}$	$\frac{1}{\chi^{\kappa(p+1)}}$
$cos(\eta\tau^{\kappa})$	$\frac{\chi^{\kappa}}{\chi^{2\kappa}+\eta^2}$
$sin(\eta\tau^{\kappa})$	$\frac{\eta^{\kappa}}{\chi^{2\kappa}+\eta^2}$

Please cite this article in press as: K.-J. Wang et al., The transient analysis for zero-input response of fractal RC circuit based on local fractional derivative, Alexandria Eng. J. (2020), https://doi.org/10.1016/j.aej.2020.08.024

Combining Eq. (3.1) and Eq. (3.2) yields the following relationship

$$i_{\kappa,C}(\tau) = C_\kappa \frac{\partial^\kappa U_{\kappa,C}(\tau)}{\partial \tau^\kappa} \tag{3.3}$$

3.2. The ND resistor

Definition 3.2. The Ohm's Law for the ND resistor is defined as

$$i_{\kappa,R}(\tau) = \frac{U_{\kappa,R}(\tau)}{R_\kappa} \tag{3.4}$$

where $U_{\kappa,R}(\tau), i_{\kappa,R}(\tau)$ and R_κ represent the ND voltage, ND current and ND resistance of the ND resistor respectively.

3.3. The Kirchhoff Voltage Laws

Kirchhoff Voltage Laws is the basic law of voltage in a circuit. The content gives that the algebraic sum of the potential difference (voltage) of all components in a closed circuit is equal to zero, which can be expressed as

$$\sum_{i=1}^{m} U_{\kappa,i} = 0. \tag{3.5}$$

4. The ZIR of fractal RC circuit described by LFD

Fig. 1 illustrated the ZIR of fractal RC circuit modeled by LFD, where the ND capacitor is charged when the switch is set at the position **s1**. After a period of charging, the circuit goes into steady state. By assuming that at the time $\tau = 0$, the switch is turned to position **s2** from position **s1**, then the following relation can be obtained

$$U_{\kappa,C_\kappa}(0_-) = U_\kappa, \tag{4.1}$$

According to the law of switch, we have

$$U_{\kappa,C_\kappa}(0_-) = U_{\kappa,C_\kappa}(0_+), \tag{4.2}$$

When $\tau \geqslant 0_+$, the ND capacitor will discharge through ND resistor once the switch turns to position s2, and generate the ZIR in the ND circuit. With the help of the Kirchhoff Voltage Laws, we have

$$-U_{\kappa,C_\kappa}(\tau) + U_{\kappa,R_{\kappa,2}}(\tau) = 0, \tag{4.3}$$

Using Eq. (3.3) can yield

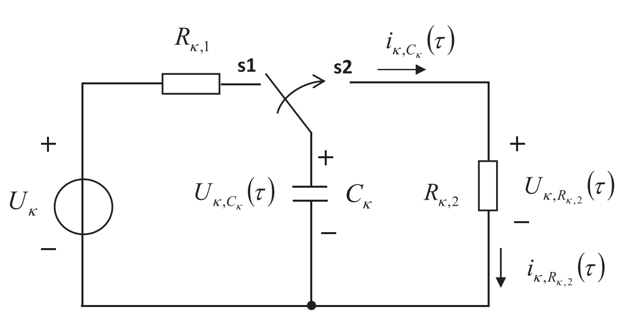

Fig. 1 The ZIR of the fractal RC circuit within LFD.

$$i_{\kappa,C_\kappa}(\tau) = -C_\kappa \frac{\partial^\kappa U_{\kappa,C_\kappa}(\tau)}{\partial \tau^\kappa}, \tag{4.4}$$

According to the series theory, there is

$$i_{\kappa,C_\kappa}(\tau) = i_{\kappa,R_{\kappa,2}}(\tau), \tag{4.5}$$

Combining Eqs. (3.4), (4.4) and (4.5), we have

$$U_{\kappa,R_{\kappa,2}}(\tau) = -R_{\kappa,2} C_\kappa \frac{\partial^\kappa U_{\kappa,C_\kappa}(\tau)}{\partial \tau^\kappa} \tag{4.6}$$

Taking Eq. (4.6) into Eq. (4.3) gives

$$-R_{\kappa,2} C_\kappa \frac{\partial^\kappa U_{\kappa,C_\kappa}(\tau)}{\partial \tau^\kappa} - U_{\kappa,C_\kappa}(\tau) = 0, \tag{4.7}$$

subject to the initial condition

$$U_{\kappa,C_\kappa}(0) = U_{\kappa,C_\kappa}(0_+) = U_\kappa. \tag{4.8}$$

where $R_{\kappa,2}$ and C_κ are constants.

Applying the LFLT to Eq. (4.7), it gives

$$R_{\kappa,2} C_\kappa \left[\chi^\kappa N_\kappa^{U_{\kappa,C_\kappa}}(\chi) - U_{\kappa,C_\kappa}(0)\right] + N_\kappa^{U_{\kappa,C_\kappa}}(\chi) = 0, \tag{4.9}$$

In this case, we can rearrange Eq. (4.9) to obtain

$$N_\kappa^{U_{\kappa,C_\kappa}}(\chi) = U_{\kappa,C_\kappa}(0) \frac{1}{\chi^\kappa + \frac{1}{R_{\kappa,2} C_\kappa}}, \tag{4.10}$$

Here we define σ_κ ($\sigma_\kappa = R_{\kappa,2} C_\kappa$) as ND time constant. By using the initial condition, Eq. (4.10) can be written as

$$N_\kappa^{U_{\kappa,C_\kappa}}(\chi) = U_\kappa \frac{1}{\chi^\kappa + \frac{1}{\sigma_\kappa}}, \tag{4.11}$$

Taking the ILFLT for Eq. (4.11), yields

$$U_{\kappa,C_\kappa}(\tau) = U_\kappa E_\kappa\left(-\frac{\tau^\kappa}{\sigma_\kappa}\right), \tag{4.12}$$

According to Eq. (4.4), the expression of $i_{\kappa,C_\kappa}(\tau)$ can be obtained

$$i_{\kappa,C_\kappa}(\tau) = \frac{U_\kappa}{R_{\kappa,2}} E_\kappa\left(-\frac{\tau^\kappa}{\sigma_\kappa}\right), \tag{4.13}$$

In accordance with Eq. (4.3), there is

$$U_{\kappa,R_{\kappa,2}}(\tau) = U_\kappa E_\kappa\left(-\frac{\tau^\kappa}{\sigma_\kappa}\right), \tag{4.14}$$

Using Eq. (3.4), we can obtain the expression of $i_{\kappa,R_{\kappa,2}}(\tau)$ as

$$i_{\kappa,R_{\kappa,2}}(\tau) = \frac{U_\kappa}{R_{\kappa,2}} E_\kappa\left(-\frac{\tau^\kappa}{\sigma_\kappa}\right), \tag{4.15}$$

5. Analysis of the ND-ZIR

Now we let $U_\kappa = 1$, $R_{\kappa,2} = 2$, $\sigma_\kappa = 1$ to study the effect of different fractional orders κ on the circuit properties, and the fractional orders we use are $\kappa = 0.2$, ln2/ln3 and 0.9, respectively. The behavior of $U_{\kappa,C_\kappa}(\tau), i_{\kappa,C_\kappa}(\tau), U_{\kappa,R_{\kappa,2}}(\tau)$ and $i_{\kappa,R_{\kappa,2}}(\tau)$ that defined on Cantor sets are illustrated in Figs. 2–5 for different fractional orders.

When observing the curves in the legend, it is not difficult to find that with the increase of fractional order κ, the value of corresponding quantity tends to increase. That is to say, when the time is fixed, the larger the fractional order is, the larger the corresponding value is. In addition, we find that Fig.2 is the

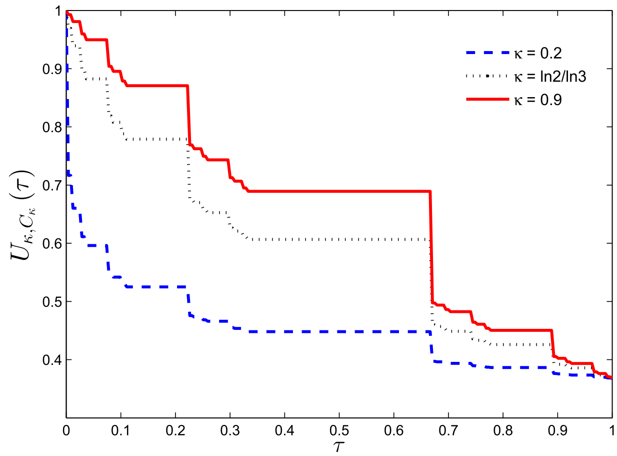

Fig. 2 The behavior of $U_{\kappa,C_\kappa}(\tau)$ for different fractional orders on Cantor sets.

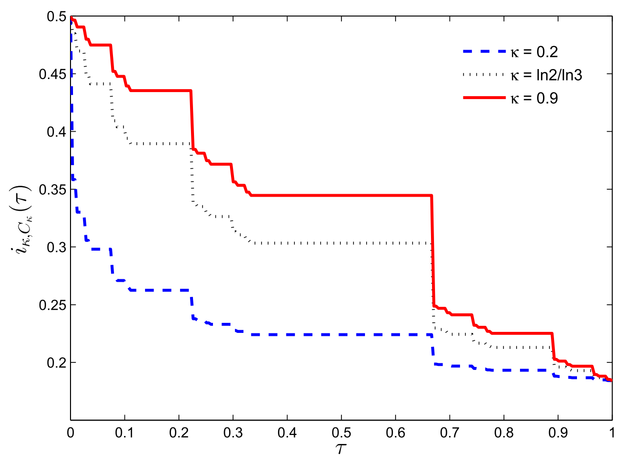

Fig. 3 The behavior of $i_{\kappa,C_\kappa}(\tau)$ for different fractional orders on Cantor sets.

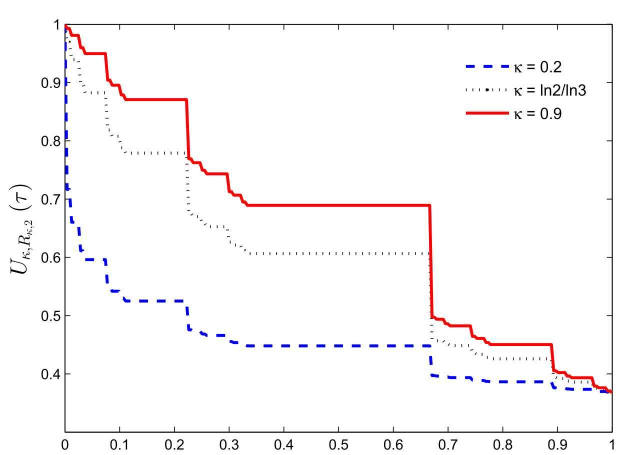

Fig. 4 The behavior of $U_{\kappa,R_{\kappa,2}}(\tau)$ for different fractional orders on Cantor sets.

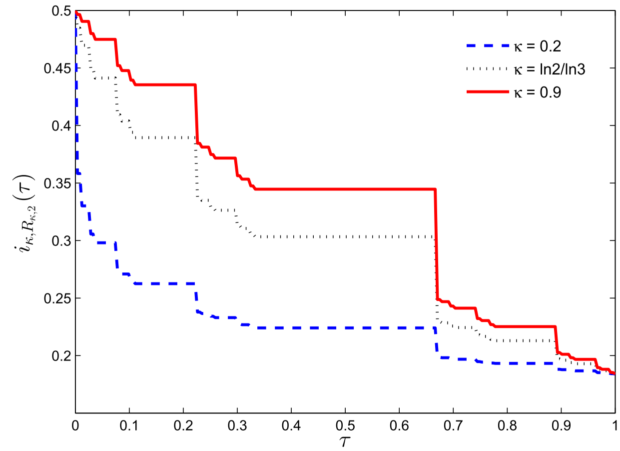

Fig. 5 The behavior of $i_{\kappa,R_{\kappa,2}}(\tau)$ for different fractional orders on Cantor sets.

same as Fig.4, this is because the algebraic sum of potential difference (voltage) of all components along the closed circuit is equal to zero. Due to the series connection between the ND resistor and ND capacitor, the results in Figs. 3 and 5 are also consistent.

Let $U_\kappa = 1$, $\kappa = \ln 2/\ln 3$, we use three different ND time constants to study the ND-ZIR, that is $\sigma_{ln2/ln3} = 1$ ($R_{ln2/ln3,2} = 1$, $C_{ln2/ln3} = 1$), $\sigma_{ln/ln3} = 4$ ($R_{ln2/ln3,2} = 2$, $C_{ln2/ln3} = 2$) and $\sigma_{ln2/ln3} = 16$ ($R_{ln2/ln3,2} = 4$, $C_{ln2/ln3} = 4$). The curves of $U_{ln2/ln3,C_{ln2/ln3}}(\tau), i_{ln2/ln3,C_{ln2/ln3}}(\tau), U_{ln2/ln3,R_{ln2/ln3,2}}(\tau)$ and $i_{ln2/ln3,R_{ln2/ln3,2}}(\tau)$ defined on Cantor sets are plotted in Figs. 6–9.

It is easily seen that the attenuation rate of the curves is related to σ_κ, the attenuation of the curves decrease with the increase of ND time constant σ_κ. As an important physical quantity, the ND time constant is generally used to measure the change speed of transient process, and it is also a physical quantity to measure the discharge speed of ND capacitor. The larger the σ_κ value is, the longer the transient process is, and the smaller the σ_κ value is, the shorter the transient process is. In the actual circuit, the speed of the transition process

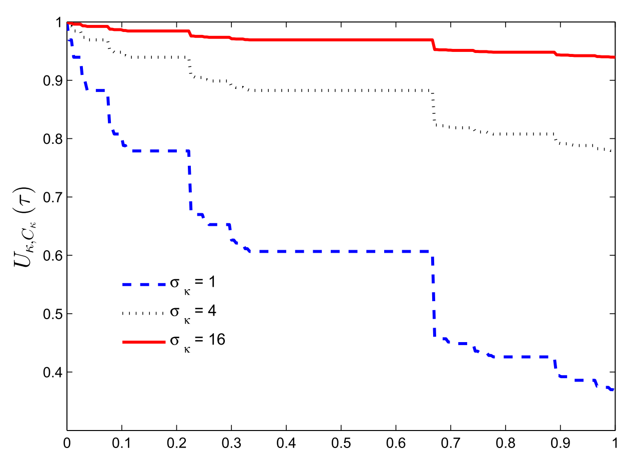

Fig. 6 The behavior of $U_{\kappa,C_\kappa}(\tau)$ with different ND time constants $\sigma_\kappa = 1, 4, 16$ at $\kappa = \ln 2/\ln 3$, $U_\kappa = 1$ defined on Cantor sets.

Please cite this article in press as: K.-J. Wang et al., The transient analysis for zero-input response of fractal RC circuit based on local fractional derivative, Alexandria Eng. J. (2020), https://doi.org/10.1016/j.aej.2020.08.024

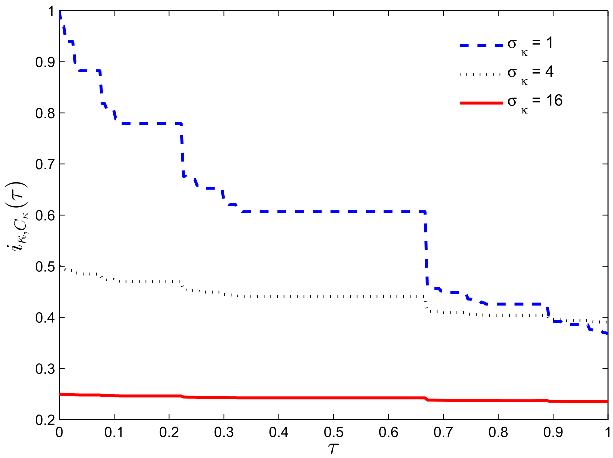

Fig. 7 The behavior of $i_{\kappa,C_\kappa}(\tau)$ with different ND time constants $\sigma_\kappa = 1, 4, 16$ at $\kappa = \ln 2/\ln 3$, $U_\kappa = 1$ defined on Cantor sets.

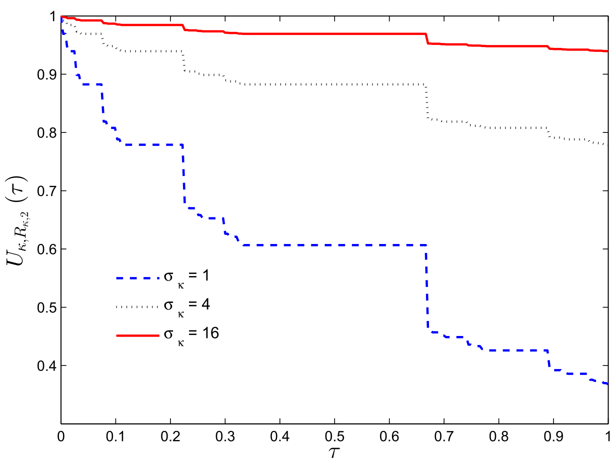

Fig. 8 The behavior of $U_{\kappa,R_{\kappa,2}}(\tau)$ with different ND time constants $\sigma_\kappa = 1, 4, 16$ at $\kappa = \ln 2/\ln 3$, $U_\kappa = 1$ defined on Cantor sets.

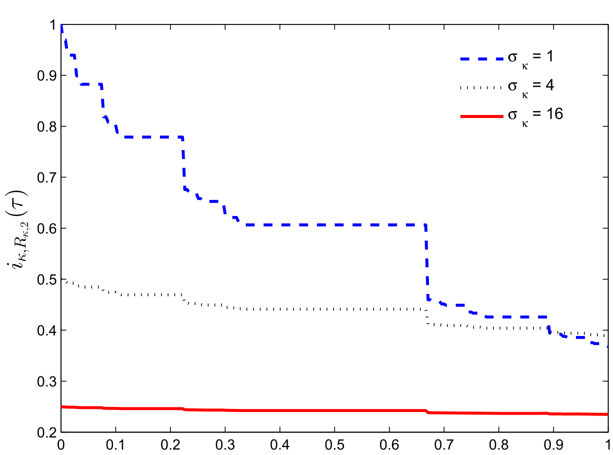

Fig. 9 The behavior of $i_{\kappa,R_{\kappa,2}}(\tau)$ with different ND time constants $\sigma_\kappa = 1, 4, 16$ at $\kappa = \ln 2/\ln 3$, $U_\kappa = 1$ defined on Cantor sets.

can be controlled by selecting the appropriate values of $R_{\kappa,2}$ and C_κ. For different ND time constants, Figs. 6 and 8 are the same, Figs. 7 and 9 are also the same, which are all determined by the physical characteristics of the circuit when the switch is on position s2.

It is worth noting that in the particular case $\kappa = 1$, the ZIR of the fractal circuit becomes the ordinary one, and the corresponding expressions of $U_{\kappa,C_\kappa}(\tau), i_{\kappa,C_\kappa}(\tau), U_{\kappa,R_{\kappa,2}}(\tau)$ and $i_{\kappa,R_{\kappa,2}}(\tau)$ are simplified as

$$U_C(\tau) = U_\kappa e^{\left(-\frac{\tau}{\sigma}\right)}, \tag{5.1}$$

$$i_C(\tau) = \frac{U_\kappa}{R_{\kappa,2}} e^{\left(-\frac{\tau}{\sigma}\right)}, \tag{5.2}$$

$$U_{\kappa,R_{\kappa,2}}(\tau) = U_\kappa e^{\left(-\frac{\tau}{\sigma}\right)}, \tag{5.3}$$

$$i_{\kappa,R_{\kappa,2}}(\tau) = \frac{U_\kappa}{R_{\kappa,2}} e^{\left(-\frac{\tau}{\sigma}\right)}, \tag{5.4}$$

When $U_\kappa = 1$, $\sigma_\kappa = 1$ ($R_{\kappa,2} = 1/2$, $C_\kappa = 1$), the curves of $U_{\kappa,C_\kappa}(\tau), i_{\kappa,C_\kappa}(\tau), U_{\kappa,R_{\kappa,2}}(\tau)$ and $i_{\kappa,R_{\kappa,2}}(\tau)$ compared between $\kappa = 1$ and $\kappa = \ln 2/\ln 3$ are shown in Figs. 10–13. Since the switch is

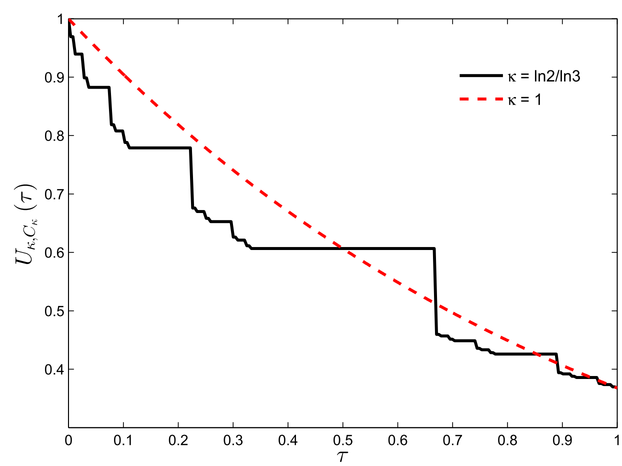

Fig. 10 The curves of $U_{\kappa,C_\kappa}(\tau)$ for $\kappa = 1$ and $\kappa = \ln 2/\ln 3$.

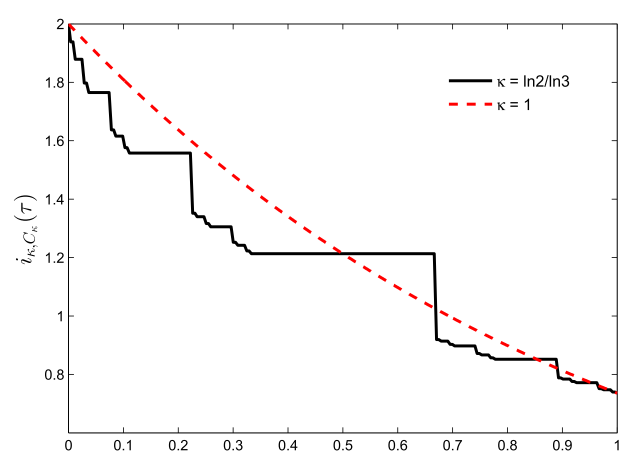

Fig. 11 The curves of $i_{\kappa,C_\kappa}(\tau)$ for $\kappa = 1$ and $\kappa = \ln 2/\ln 3$.

Please cite this article in press as: K.-J. Wang et al., The transient analysis for zero-input response of fractal RC circuit based on local fractional derivative, Alexandria Eng. J. (2020), https://doi.org/10.1016/j.aej.2020.08.024

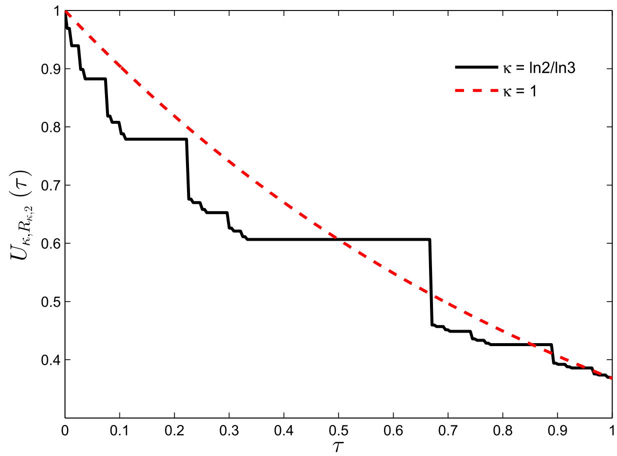

Fig. 12 The curves of $U_{\kappa,R_{\kappa,2}}(\tau)$ for $\kappa = 1$ and $\kappa = \ln 2/\ln 3$.

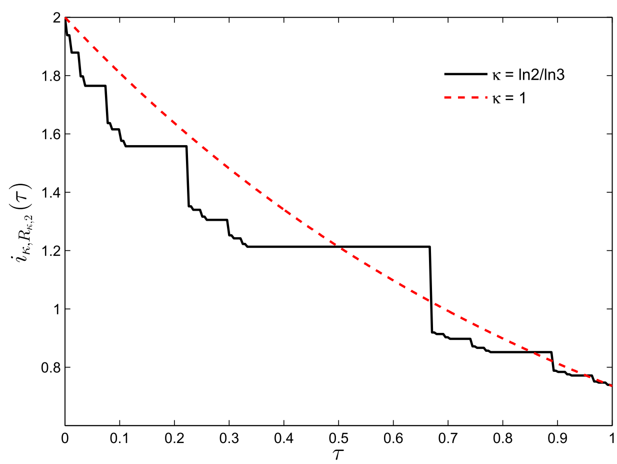

Fig. 13 The curves of $i_{\kappa,R_{\kappa,2}}(\tau)$ for $\kappa = 1$ and $\kappa = \ln 2/\ln 3$.

turned to position 2, only ND resistor and ND capacitor constitute a closed circuit in series, which lead to the results in Figs. 10 and 12 remain the same as well as that of Figs. 11 and 13.

6. Conclusion

We have successfully modeled the ZIR of the fractal RC circuit by LFD in this paper for the first time, where the transient local fractional ordinary differential equation is obtained with aid of the law of switch and Kirchhoff Voltage Laws. The exact solution defined on Cantor sets is given by using the LFLT and ILFLT, and the ND time constant is elaborated as well. It is found that the ZIR of fractal RC circuit converts into the ordinary one in the particular case $\kappa = 1$. The obtained results are expected to open some new perspectives towards the characterization of ND electric circuits via LFD.

Declaration of Competing Interest

The authors declare that they have no known competing financial interests or personal relationships that could have appeared to influence the work reported in this paper.

Acknowledgment

This work is supported by Program of Henan Polytechnic University (No. B2018-40).

References

[1] Samir Ladaci, Abdelfatah Charef, On fractional adaptive control, Nonlinear Dyn. 43 (4) (2006) 365–378.
[2] B. Yu, P. Cheng, A fractal permeability model for bi-dispersed porous media, Int. J. Heat Mass Transf. 45 (14) (2002) 2983–2993.
[3] B. Yu, P. Cheng, Fractal models for the effective thermal conductivity of bidispersed porous media, J. Thermophys. Heat Transf. 16 (1) (2002) 22–29.
[4] T. Miao, Z. Long, A. Chen, et al, Analysis of permeabilities for slug flow in fractal porous media, Int. Commun. Heat Mass Transf. 88 (2017) 194–202.
[5] D. Kumar, J. Singh, K. Tanwar, et al, A new fractional exothermic reactions model having constant heat source in porous media with power, exponential and Mittag-Leffler laws, Int. J. Heat Mass Transf. 138 (2019) 1222–1227.
[6] Pedram Ghamisi et al, An efficient method for segmentation of images based on fractional calculus and natural selection, Expert Syst. Appl. 39 (16) (2012) 12407–12417.
[7] B. Yu, J. Li, Some fractal characters of porous media, Fractals 9 (03) (2001) 365–372.
[8] A. Goswami, J. Singh, D. Kumar, et al, An efficient analytical approach for fractional equal width equations describing hydro-magnetic waves in cold plasma, Physica A 524 (2019) 563–575.
[9] A. Atangana, On the new fractional derivative and application to nonlinear Fishers reaction-diffusion equation, Appl. Math. Comput. 273 (2016) 948–956.
[10] D. Kumar, J. Singh, D. Baleanu, On the analysis of vibration equation involving a fractional derivative with Mittag-Leffler law, Math. Meth. Appl. Sci. 43 (1) (2020) 443–457.
[11] D. Kumar, J. Singh, New aspects of fractional epidemiological model for computer viruses with Mittag-Leffler law, mathematical modelling in health, Soc. Appl. Sci. (2020) 283–301.
[12] D. Baleanu, H. Khan, H. Jafari, R.A. Khan, On the exact solution of wave equations on cantor sets, Entropy 17 (9) (2015) 6229–6237.
[13] S. Bhatter, A. Mathur, D. Kumar, J. Singh, A new analysis of fractional Drinfeld-Sokolov-Wilson model with exponential memory, Physica A 537 (2020) 122578.
[14] V.P. Dubey, R. Kumar, D. Kumar, I. Khan, J. Singh, An efficient computational scheme for nonlinear time fractional systems of partial differential equations arising in physical sciences, Adv. Differ. Equ. 1 (2020) 46.
[15] X.J. Yang, J.A.T. Machado, A new fractional operator of variable order: application in the description of anomalous diffusion, Physica A 481 (2017) 276–283.
[16] D. Kumar, J. Singh, M. Al Qurashi, D. Baleanu, A new fractional SIRS-SI malaria disease model with application of vaccines, antimalarial drugs, and spraying, Adv. Differ. Equ. 1 (2019) 278.
[17] W.B. Sun, Some local fractional integral inequalities for generalized preinvex functions and applications to numerical quadrature, Fractals 27 (5) (2019).
[18] K.L. Wang, K.J. Wang, A modification of the reduced differential transform method for fractional calculus, Therm. Sci. 22 (4) (2018) 1871–1875.
[19] J.H. He et al, A new fractional derivative and its application to explanation of polar bear hairs, J. King Saud Univ. Sci. 28 (2) (2016) 190–192.
[20] X.J. Yang, General fractional calculus operators containing the generalized Mittag-Leffler functions applied to anomalous relaxation[J], Therm. Sci. 21 (suppl. 1) (2017) 317–326.

[21] J.H. He, F.Y. Ji, Two-scale mathematics and fractional calculus for thermodynamics, Therm. Sci. 23 (4) (2019) 2131–2133.
[22] J.H. He, Fractal calculus and its geometrical explanation, Res. Phys. 10 (2018) 272–276.
[23] M.R.S. Ammi, I. Jamiai, D.F.M. Torres, A finite element approximation for a class of Caputo time-fractional diffusion equations, Comput. Math. Appl. 78 (5) (2019) 1334–1344.
[24] X.J. Yang, J.A. TenreiroMachado, D. Baleanu, C. Cattani, On exact traveling-wave solutions for local fractional Korteweg-de Vries equation, Chaos Interdiscip. J. Nonlinear Sci. 26 (8) (2016) 084312.
[25] X.J. Yang, F. Gao, H.M. Srivastava, New rheological models within local fractional derivative, Rom. Rep. Phys. 69 (3) (2017) 113.
[26] X.J. Yang, J.A.T. Machado, C. Cattani, et al, On a fractal LC-electric circuit modeled by local fractional calculus, Commun. Nonlinear Sci. Numer. Simul. 47 (2017) 200–206.
[27] X.H. Zhao, Y. Zhang, D. Zhao, et al, The RC circuit described by local fractional differential equations, Fundamenta Informaticae 151 (1–4) (2017) 419–429.
[28] X.J. Yang, J.A. Tenreiro Machado, A new fractal nonlinear Burgers' equation arising in the acoustic signals propagation, Math. Meth. Appl. Sci. 42 (18) (2019) 7539–7544.
[29] X.J. Yang, J.A.T. Machado, D. Baleanu, Exact traveling-wave solution for local fractional Boussinesq equation in fractal domain, Fractals 25 (04) (2017) 1740006.
[30] Yu. Zhang, X.J. Yang, An efficient analytical method for solving local fractional nonlinear PDEs arising in mathematical physics, Appl. Math. Model. 40 (3) (2016) 1793–1799.
[31] X.J. Yang, H.M. Srivastava, An asymptotic perturbation solution for a linear oscillator of free damped vibrations in fractal medium described by local fractional derivatives, Commun. Nonlinear Sci. Numer. Simul. 29 (1–3) (2015) 499–504.
[32] K.J. Wang, On a High-pass filter described by local fractional derivative, Fractals 28 (03) (2020) 2050031.
[33] X.J. Yang, F. Gao, H.M. Srivastava, A new computational approach for solving nonlinear local fractional PDEs, J. Comput. Appl. Math. 339 (2018) 285–296.
[34] X.J. Yang, F. Gao, H.M. Srivastava, Exact travelling wave solutions for the local fractional two-dimensional Burgers-type equations, Comput. Math. Appl. 73 (2) (2017) 203–210.
[35] X.J. Yang, F. Gao, H.M. Srivastava, Non-differentiable exact solutions for the nonlinear ODEs defined on fractal sets, Fractals 25 (04) (2017) 1740002.
[36] K.L. Wang, K.J. Wang, C.H. He, Physical insight of local fractional calculus and its application to fractional Kdv-Burgers equation, Fractal 27 (7) (2019), 1950122-777.
[37] X.J. Yang, J.A. Machado, D. Baleanu, et al., A new numerical technique for local fractional diffusion equation in fractal heat transfer, J. Nonlinear Sci. Appl. 9(10) (2016) 5621–5628.
[38] K.L. Wang, S.W. Yao, Y.P. Liu, et al, A fractal variational principle for the telegraph equation with fractal derivatives, Fractals 28 (4) (2020) 2050058.
[39] X.J. Yang, D. Baleanu, H.M. Srivastava, Local Fractional Integral Transforms and their Applications, Academic Press, Elsevier, 2015.